

# Unexpected B<sub>II</sub> Conformer Substate Population in Unoriented Hydrated Films of the d(CGCGAATTCGCG)<sub>2</sub> Dodecamer and of Native B-DNA from Salmon Testes

Arthur Pichler,\* Simon Rüdiger,\* Martin Mitterböck,\* Christian G. Huber,# Rudolf H. Winger,\* Klaus R. Liedl,\* Andreas Hallbrucker,\* and Erwin Mayer\*

\*Institut für Allgemeine, Anorganische und Theoretische Chemie, and #Institut für Analytische Chemie und Radiochemie, Universität Innsbruck, A-6020 Innsbruck, Austria

**ABSTRACT** Conformational substates of B-DNA had been observed so far in synthetic oligonucleotides but not in naturally occurring highly polymeric B-DNA. Our low-temperature experiments show that native B-DNA from salmon testes and the d(CGCGAATTCGCG)<sub>2</sub> dodecamer have the same B<sub>I</sub> and B<sub>II</sub> substates. Nonequilibrium distribution of conformer population was generated by quenching hydrated unoriented films to 200 K, and isothermal structural relaxation toward equilibrium by interconversion of substates was followed by Fourier transform infrared spectroscopy. B<sub>I</sub> interconverts into B<sub>II</sub> on isothermal relaxation at 200 K, whereas on slow cooling from ambient temperature, B<sub>II</sub> interconverts into B<sub>I</sub>. Our estimation of the dodecamer's B<sub>I</sub>-to-B<sub>II</sub> conformer substate population by curve resolution of the symmetrical stretching vibration of the ionic phosphate is  $2.4 \pm 0.5$  to 1 at 200 K, and it is  $1.3 \pm 0.5$  to 1 between 270 and 290 K. Pronounced spectral changes upon B<sub>I</sub>-to-B<sub>II</sub> interconversion are consistent with base destacking coupled with migration of water from ionic phosphate toward the phosphodiester and sugar moieties. Nonspecific interaction of proteins with the DNA backbone could become specific by induced-fit-type interactions with either B<sub>I</sub> or B<sub>II</sub> backbone conformations. This suggests that the B<sub>I</sub>-to-B<sub>II</sub> substate interconversion could be a major contributor to the protein recognition process.

## INTRODUCTION

In the known protein-DNA complexes, about half of the hydrogen bonds involve contacts with the DNA sugar-phosphate backbone (Pabo and Sauer, 1992; Travers, 1994; Luisi, 1995). The exact role of backbone contacts is not known. Two major roles discussed are that backbone contacts help to anchor the protein in a fixed arrangement and that contacts with the DNA backbone may allow indirect recognition of the sequence (Pabo and Sauer, 1992). A particular local conformation of the DNA seems to be essential for favorable interaction with a protein (Travers, 1994), and thus conformational substates (CSs) of biologically active B-DNA could play a decisive role. In single crystals of synthetic B-type oligonucleotides, the dominant phosphodiester backbone conformation (B<sub>I</sub>) is the same as that proposed by modeling studies of oriented fibers of native canonical B-DNA (Fratini et al., 1982; Kopka et al., 1983; Cruse et al., 1986; Privé et al., 1987; Grzeskowiak et al., 1991; Arnott et al., 1975). A minor backbone conformation (B<sub>II</sub>) observed so far only in oligonucleotides was only attributed to crystal packing effects (Dickerson et al., 1987). The B<sub>I</sub> and B<sub>II</sub> CSs involve changes in the phosphate backbone conformation about the C3'-O3'-P segment of the backbone chain (Fratini et al., 1982; Cruse et al., 1986; Privé et al., 1987; Grzeskowiak et al., 1991). These CSs are

frozen-in in the crystal but interconvert in solution at ambient temperature on a (sub)nanosecond time scale (Hogan and Jardetzky, 1979; Chou et al., 1992; Gorenstein, 1994). Conformational deviations within the B family of DNA were observed by Raman (Peticolas, 1995) and solid-state <sup>31</sup>P-NMR spectroscopy (Song et al., 1997). Peticolas (1995) pointed out that "this conformational variability may play an important role in protein-DNA recognition in addition to the primary mechanism of recognition by the array of hydrogen bond donors and acceptors presented by a sequence of bases."

Here we show that native B-DNA from salmon testes, with a base pair length from ~400 to >5000, and the d(CGCGAATTCGCG)<sub>2</sub> dodecamer (containing an *Eco*RI restriction site) have the same B<sub>I</sub> and B<sub>II</sub> substates. The distinct infrared spectral features of the two substates are obtained by a new method in which nonequilibrium conformer population is generated by rapid quenching of an unoriented hydrated film into the glassy state (Rüdiger, 1997; Rüdiger et al., 1997b). On subsequent heating into the glass→liquid transition region (Rüdiger et al., 1996; Rüdiger et al., 1997a), interconversion of conformers on relaxation toward equilibrium is followed isothermally by Fourier transform infrared (FT-IR) spectroscopy. Pronounced spectral changes at 200 K on B<sub>I</sub>-to-B<sub>II</sub> interconversion are consistent with base destacking coupled with migration of water from ionic phosphate toward the phosphodiester and sugar moieties. The assignment of these spectral changes to the B<sub>I</sub> and B<sub>II</sub> conformer substate is consistent with a recent state-of-the-art molecular dynamics (MD) simulation of the d(CGCGAATTCGCG)<sub>2</sub> dodecamer in aqueous solution, where changes in the hydration shells

Received for publication 21 May 1998 and in final form 20 April 1999.

Address reprint requests to Dr. Erwin Mayer, Institut für Allgemeine, Anorganische und Theoretische Chemie, Leopold-Franzens Universität Innsbruck, A-6020, Innrain 52a, Innsbruck, Austria. Tel.: 43-512-507-5110; Fax: 43-512-507-2934; E-mail: erwin.mayer@uibk.ac.at.

© 1999 by the Biophysical Society

0006-3495/99/07/398/12 \$2.00

on B<sub>I</sub>-to-B<sub>II</sub> transition have been attributed to migration of water from ionic phosphate toward the sugar oxygen (Winger et al., 1998).

Curve resolution of the infrared spectra recorded at 200 K and at ambient temperature allows us to determine the B<sub>I</sub>-to-B<sub>II</sub> conformer substate population. This estimation gives  $2.4 \pm 0.5:1$  at 200 K, and  $1.3 \pm 0.5:1$  between 270 and 290 K. Therefore, the B<sub>II</sub> substate population is considerably higher in the unoriented dodecamer than in the crystal, where a B<sub>I</sub>-to-B<sub>II</sub> substate population ratio of 10:1 has been observed (Fratini et al., 1982; Privé et al., 1987; Grzeskowiak et al., 1991). Consequently, nonspecific interaction of proteins with the DNA backbone could become specific by induced-fit-type interactions with either B<sub>I</sub> or B<sub>II</sub> backbone conformations (Spolar and Record, 1994). This suggests that the B<sub>I</sub>-to-B<sub>II</sub> substate interconversion could be a major contributor to the protein-DNA recognition process.

Our infrared spectroscopic study is consistent with the comparison by Kubasek et al. (1986) of the d(CGCGAATTCGCG)<sub>2</sub> dodecamer Raman spectra with those of purified DNA from salmon sperm and the DNA inside the intact salmon sperm head. Kubasek et al. (1986) conclude "that the average conformation of these nucleic acids must be very similar" because bands occur at very similar frequencies but with slightly altered intensities.

## MATERIALS AND METHODS

### Materials

The lyophilized d(CGCGAATTCGCG)<sub>2</sub> dodecamer was obtained as sodium salt from MWG BIOTECH, after purification by high-performance liquid chromatography. The triethylammonium acetate buffer was removed quantitatively by repeated precipitation of the dodecamer from aqueous solution with cold ethanol. Quantitative removal of the buffer was confirmed by the absence of the intense buffer bands at 1558 and 1414 cm<sup>-1</sup>. Films of hydrated unoriented d(CGCGAATTCGCG)<sub>2</sub> were obtained by keeping the aqueous solutions on AgCl discs over saturated KCl or KNO<sub>3</sub> solution for several days. The hydrated d(CGCGAATTCGCG)<sub>2</sub> films were thereafter covered with a second AgCl disc, the two discs were taped, and the sample was positioned in a homemade copper holder for the cryostat. Special care was taken to avoid orientation of the film, and the method of preparation ensures unoriented films. Sample and sample holder were quenched to ~170 K at a rate of ~60 K min<sup>-1</sup> into the glassy state inside the cryostat, by forcing liquid N<sub>2</sub> through the cooling tubes of the sample holder. This method of quenching differs from that described before (Rüdiger et al., 1997b), but because the cooling rate was sufficient to generate nonequilibrium population of conformers, it was preferred because it gives a more stable background in the infrared spectra. To avoid dehydration of the film, a pressure of ~600 mbar of N<sub>2</sub> was maintained during the whole experiment. A baffle cooled to ~100 K with cold N<sub>2</sub> was inserted in the vacuum line. This quantitatively removes water vapor in the apparatus and thus makes its subtraction in the infrared spectra unnecessary.

The base pair length of NaDNA from salmon testes (sodium salt from Fluka; no. 31163) was determined according to the method of Huber et al. (1995). The DNA molecular weight marker XVII (from Boehringer-Mannheim, 500 bp ladder, from 500 to 5000 bp) was used as the standard. The broad distribution of lengths ranged from ~400 to >5000 bp.

### Infrared spectra

Infrared spectra were recorded in transmission on a Biorad model FTS-45 at 4 cm<sup>-1</sup> resolution by coadding 64 scans (UDRI, DTGS detector;

zero-filling factor 2; low-pass filter at 1.12 kHz; triangular apodization). The collection time of 150 s constitutes the time resolution. The spectra are displayed in the figures on the same ordinate scales. Vertical bars indicate the ordinate scale in absorbance units. The infrared spectra of the films were first recorded at several temperatures between 290 and 260 K to characterize the films and their hydration. The spectra were very similar to that reported for the single crystal (Taillandier, 1990). The  $\Gamma$  values (water molecules per nucleotide) of the films were determined from the ratios of the measured absorbance at 3400 cm<sup>-1</sup> (due to OH groups) and at ~1220 cm<sup>-1</sup> (due to phosphate groups) of DNA (Falk et al., 1962b). Infrared spectra of the quenched films were recorded isothermally thereafter at selected temperatures (constant to  $\pm 0.1^\circ$ ), and spectral changes were followed in the form of difference spectra recorded at the same temperature to avoid temperature-dependent changes in band profiles. For the film with  $\Gamma = 13$ , the absence of ice formation was controlled in the OH stretching band region (Falk et al., 1970). The absence of dehydration or irreversible spectral changes was confirmed by comparing infrared spectra recorded at 290 K before and after the low-temperature experiment. Reproducibility of the spectral features was ascertained at 200 K with the  $\Gamma = 13$  film. SpecFit Software was used to determine the number of principal components by principal component analysis.

### Curve resolution

Curve resolution was applied with a sum of Gaussian and Lorentzian peak shapes (GRAMS/32 software; Galactic Industries Corp.). Reliable curve resolution of the spectral region from 1155 to 995 cm<sup>-1</sup> was accomplished as described by Fleissner et al. (1996), by comparison of the second derivative of the experimental composite band profile with that of the sum of the curve-fitted component bands. As a further criterion for reliability of our curve fits, we used the comparison of the experimental difference curves with that of the difference curves generated by subtraction of sums of curve-fitted component bands, aiming again for optimal correspondence between the two difference curves. The slightly sloping background in the original spectra was corrected by two-point base line subtraction, with break points set at 1155 and 995 cm<sup>-1</sup>. Second derivatives are shown inverted, and 11-point second-derivative convolution was applied throughout.

Peak shapes of the curve-fitted component bands were in all cases nearly pure Gaussian, although the band shape has not been fixed at the beginning of the fit. Infrared band shapes are Lorentzian according to a simple model in which only pressure broadening is considered. However, in real samples a further line broadening mechanism exists, and "the true line shape then is some combination of Lorentzian and Gaussian shapes" (Saarinen et al., 1995). Seshadri and Jones (1963) argue that on solute-solvent interaction, "one might expect that the bands associated with such systems would be more pronouncedly of Gauss form because the number of participating species will be very large." In our previous curve resolution studies of contact ion pairing in glassy aqueous solution, the band shapes were nearly pure Gaussian (Fleissner et al., 1996, 1998).

### Relaxation times

The time dependence at 200 K was evaluated for the B-DNA film from salmon testes, with  $\Gamma = 12$ , by exponentially fitting the spectral changes in the form of second derivatives of the difference curves. Relaxation times in minutes, with errors in brackets, of several selected bands are (for B<sub>I</sub>) 36(2) for 1720 cm<sup>-1</sup>, 27(2) for 1209 cm<sup>-1</sup>, 27(1) for 1085 cm<sup>-1</sup>, 38(1) for 1052 cm<sup>-1</sup>, 35(1) for 976 cm<sup>-1</sup>, 31(3) for 941 cm<sup>-1</sup>, 40(4) for 903 cm<sup>-1</sup>; and (for B<sub>II</sub>) 36(1) for 1243 cm<sup>-1</sup>, 26(1) for 1101 cm<sup>-1</sup>, 44(2) for 1064 cm<sup>-1</sup>, 41(3) for 959 cm<sup>-1</sup>, and 35(5) for 886 cm<sup>-1</sup>. Peak positions are those shown in Fig. 2; relaxation times are from Rüdiger (1997) and Rüdiger et al. (1997b).

## RESULTS

### Isothermal conformer interconversion in the glass→liquid transition region

To detect the infrared spectral features of the distinct  $B_I$  and  $B_{II}$  CSs of the  $d(\text{CGCGAATTCGCG})_2$  dodecamer, we first generated a nonequilibrium distribution of conformer population by quenching a hydrated unoriented film into the glassy state (Rüdiger, 1997; Rüdiger et al., 1996, 1997a,b). A hydration level of  $\Gamma = 13$  was chosen, where formation of ice can be excluded (Falk et al., 1970). We then followed structural relaxation toward equilibrium by interconversion of CSs by FT-IR spectroscopy. At 200 K relaxation occurred on time scales between minutes and hours. Therefore, interconversion of CSs can be followed easily by conventional FT-IR spectroscopy. Fig. 1 shows infrared spectra of a dodecamer film with 13 water molecules per nucleotide (that is,  $\Gamma = 13$ ) recorded at 200 K after 1 and 63 min (curves *a* and *b*). Their difference ( $b - a$ ) reveals spectral changes on isothermal relaxation, positive peaks indicating formation of a CS, and negative peaks indicating its disappearance. The decrease in intensity from the disappearing CS is clearly observable for several peaks; this is marked by arrows (Fig. 1). The increase in intensity from

the newly formed CS, however, is barely recognizable. It becomes observable only in the form of increased intensity on the wings of the main peaks. This is the first indication that the conformer substate population of the disappearing CS is higher than that of the formed CS.

Principal component analysis (PCA) was applied to a set of spectra recorded at 200 K at selected times, and it indicated only two principal components. This is consistent with our observation of isobestic points at several of the overlapping composite bands, for example at  $1225\text{ cm}^{-1}$ , which is in the region of the antisymmetrical stretching vibration of the ionic phosphate,  $\nu_{\text{as}}$ , and at  $1092\text{ cm}^{-1}$ , which is in the region of its symmetrical stretching vibration,  $\nu_s$ . These and the following assignments are made in accordance with those reported in the literature (see, e.g., Parker, 1983; Taillandier and Liquier, 1992; Cao et al., 1995; Liquier and Taillandier, 1996; Guan and Thomas, 1996a).

The spectral changes of the same dodecamer film on isothermal annealing at 200 K are shown next for several other annealing times in the form of difference curves (Fig. 2, *top*) and compared with those of a film of unoriented, highly polymeric native B-DNA from salmon testes of similar hydration ( $\Gamma = 12$ ) (Fig. 2, *bottom*; from Rüdiger et

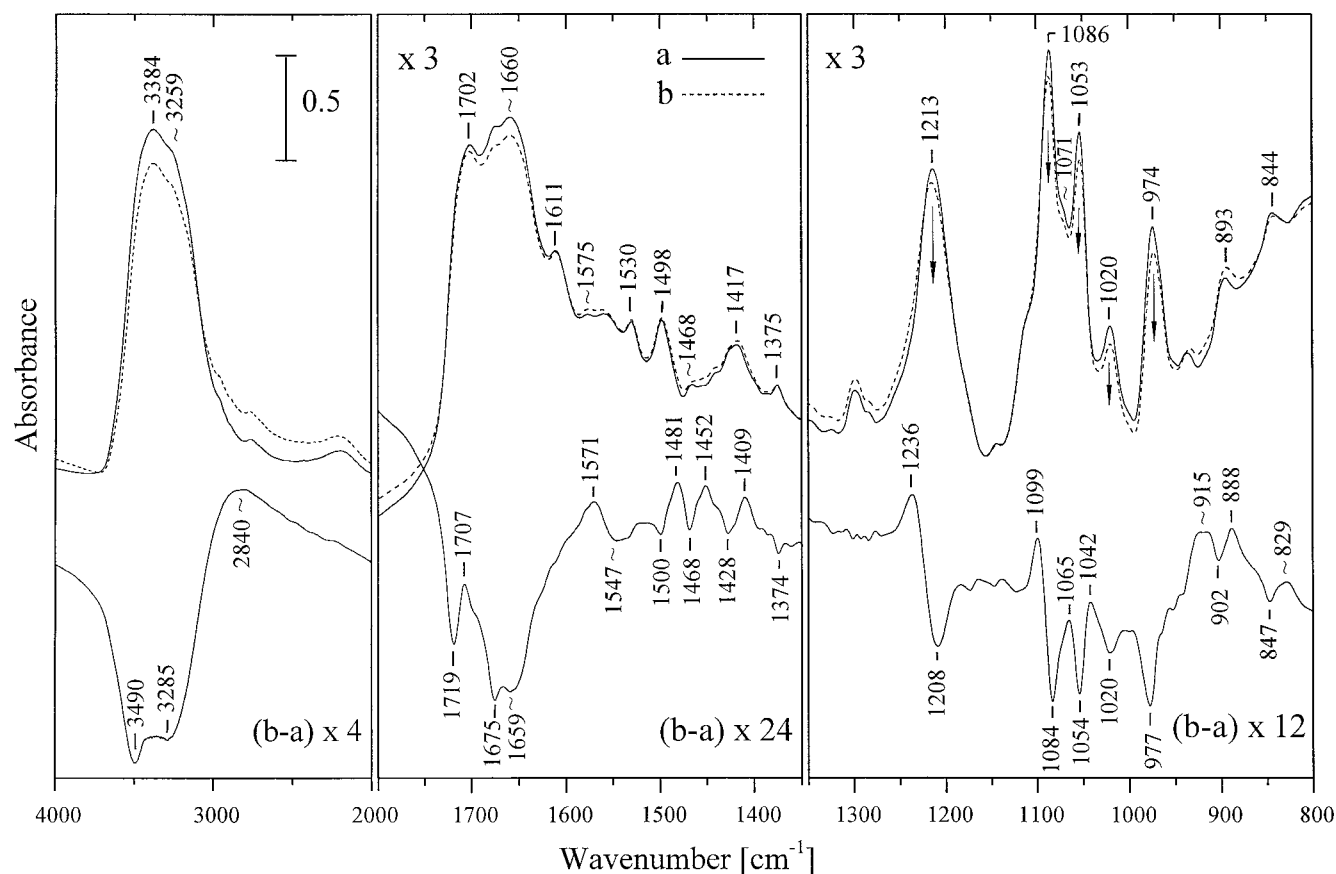


FIGURE 1 (Top) Structural relaxation by conformer interconversion as seen in infrared spectra of a quenched  $d(\text{CGCGAATTCGCG})_2$  dodecamer film with  $\Gamma = 13$  on isothermal annealing at 200 K. (a) After 1 min (—), (b) after 63 min (---). Arrows indicate decrease of band intensity. (Bottom) Difference spectrum ( $b - a$ ). The spectra are drawn on the same scale, with the enlargement factors given in the figure.

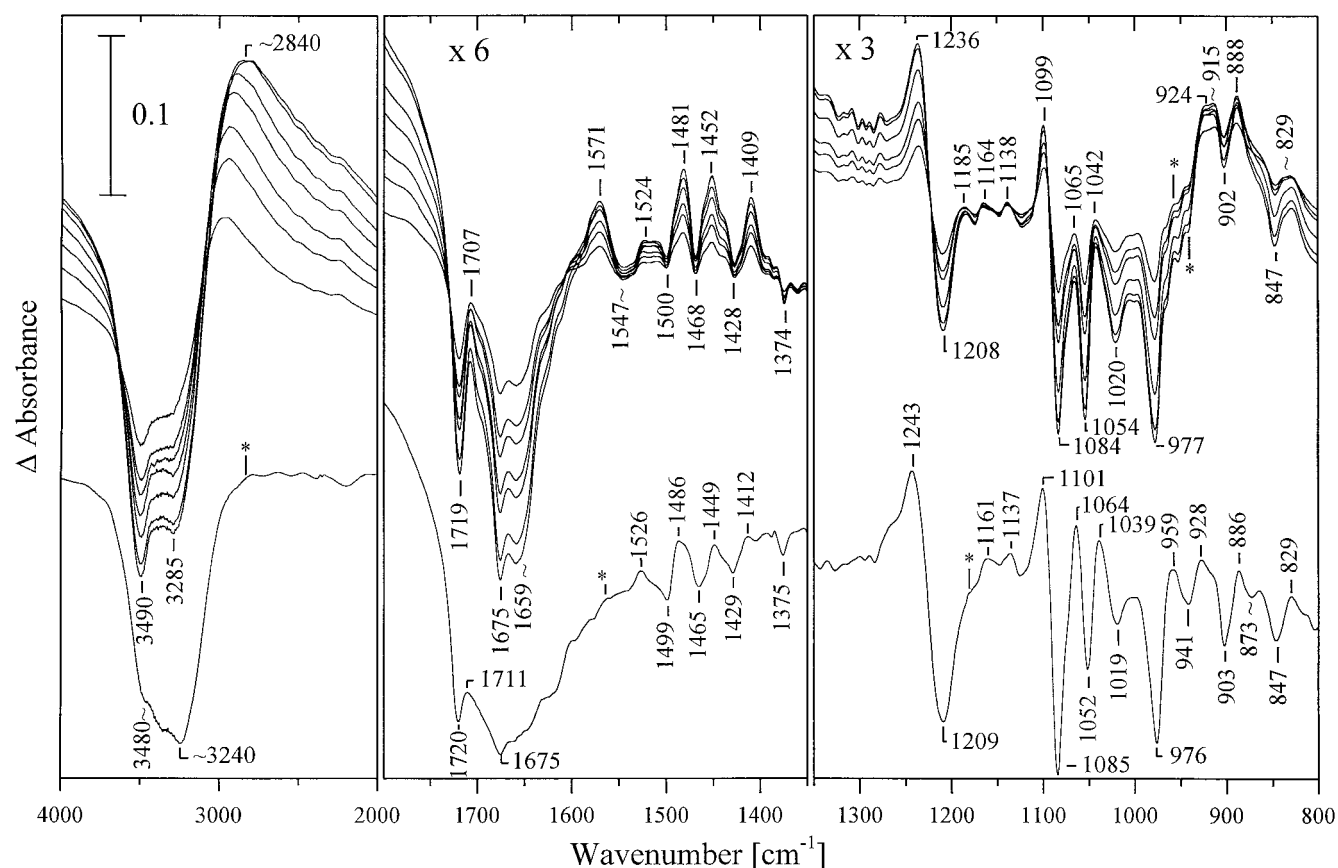


FIGURE 2 (Top) Difference curves of a quenched d(CGCGAATTCGCG)<sub>2</sub> dodecamer film with  $\Gamma = 13$ , where the spectrum recorded at 200 K after 1 min had been subtracted from that recorded after  $n$  min ( $n = 4, 7, 10, 17, 25, 49, 63$  min, respectively). (Bottom) The difference curve of a film of DNA from salmon testes, with  $\Gamma = 12$ , where the spectrum recorded at 200 K after 1 min was subtracted from that after 72 min (from figure 1 of Rüdiger et al., 1997b). Asterisks indicate the spectral region with differences between the two DNA films. The spectral changes are drawn on the same scale, enlarged sixfold (middle) and threefold (right). The sloping background caused by base line instability was partially corrected by shifting difference spectra vertically until, at 1358 (middle) and 1154  $\text{cm}^{-1}$  (right), the same absorbance value was obtained.

al., 1997b). These hydration levels were selected to exclude the formation of ice (Falk et al., 1970). Increase in annealing time affected only the intensity of the difference curves of the dodecamer film, but not band shapes or peak positions. This indicates that only interconversion of one CS into another CS has to be considered, and it is consistent with our observation of only two principal components from PCA.

The overall appearance of the dodecamer's difference curves and that of the one obtained with B-DNA from salmon testes are remarkably similar. Corresponding band positions vary at most by a few wavenumbers. For example, in the dodecamer difference spectrum, the negative feature at 1208  $\text{cm}^{-1}$ , assignable to  $\nu_{\text{as}}$  of the ionic phosphate, shifts on CS interconversion to 1236  $\text{cm}^{-1}$ , and in the difference spectrum of B-DNA from salmon testes the corresponding peak positions are at 1209 and 1243  $\text{cm}^{-1}$ . In the same manner, the negative peak in the dodecamer difference spectrum at 1084  $\text{cm}^{-1}$ , assignable to  $\nu_{\text{s}}$  of the ionic phosphate, shifts on CS interconversion to 1099  $\text{cm}^{-1}$ , and the corresponding changes in the difference spectrum obtained with B-DNA from salmon testes are at 1085 and 1101

$\text{cm}^{-1}$ , respectively. This assignment is consistent with spectral changes in a deuterated film of the dodecamer, where the negative and positive peak are also at 1084 and 1099  $\text{cm}^{-1}$  (not shown).

### Conformer substate interconversion at ambient temperatures

We next compare in Fig. 3 the isothermal difference curves obtained with the dodecamer and B-DNA from salmon testes, with difference curves obtained from spectra recorded at two different temperatures. Curves A and B are the difference curves obtained on isothermal CS interconversion at 200 K with the d(CGCGAATTCGCG)<sub>2</sub> dodecamer and B-DNA from salmon testes ( $\Gamma = 13$  and 12). Curves C and D are the 270–290 K difference curves obtained with the dodecamer and B-DNA from salmon testes ( $\Gamma = 14$  and 20). The spectral region is shown only from 1300 to 800  $\text{cm}^{-1}$ , because outside of this region pronounced changes in the band shapes of the water bands occur with changes in temperature, which lead to artefacts in the difference spectra.

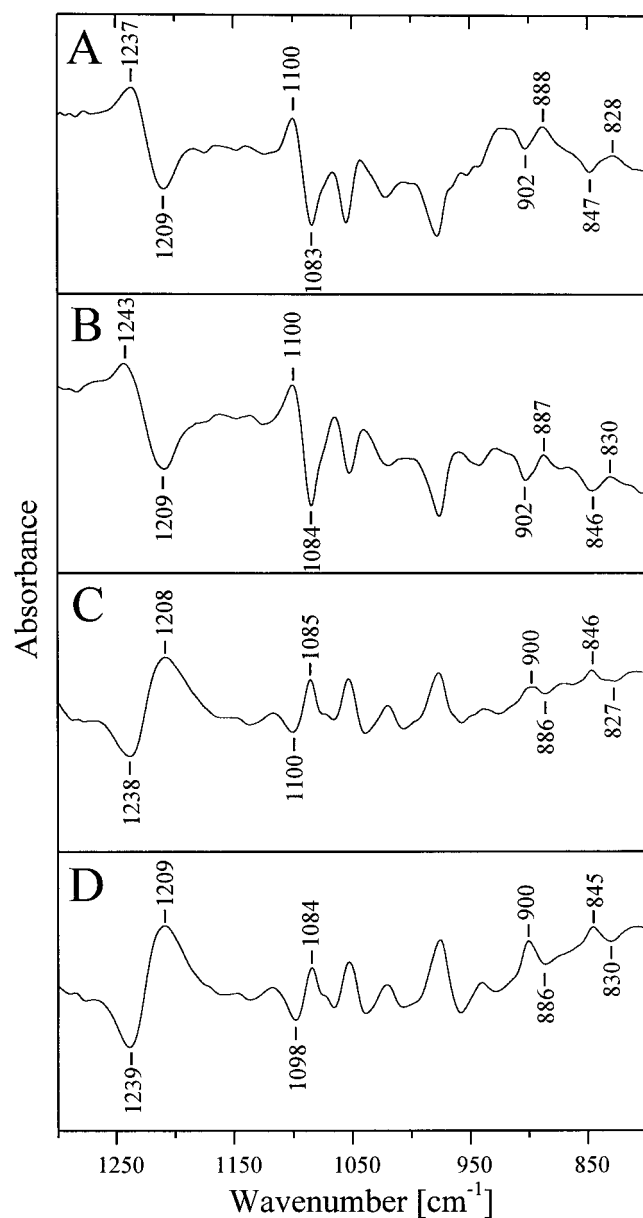


FIGURE 3 Comparison of difference curves (from 1300 to 800  $\text{cm}^{-1}$ ) obtained on isothermal annealing (A and B), with those obtained from spectra recorded at different temperatures (C and D). (A) The difference curve obtained by subtracting the spectrum of a quenched  $\text{d}(\text{CGCGAATTCGCG})_2$  film ( $\Gamma = 13$ ) recorded at 200 K after 4 min from that recorded after 25 min. (B) The corresponding difference curve from DNA from salmon testes ( $\Gamma = 12$ , 200 K, 26–4 min). (C) The difference curve from a  $\text{d}(\text{CGCGAATTCGCG})_2$  film ( $\Gamma = 14$ ) obtained by subtracting the spectrum recorded at 290 K from that at 270 K. (D) The corresponding difference curve from DNA from salmon testes ( $\Gamma \approx 20$ , 270–290 K). Note the mirror image between A and C on the one hand and B and D on the other.

The comparison in Fig. 3 demonstrates that curves C and D are on the whole the mirror images of curves A and B, and that the positive and negative band positions are very similar. This indicates, first, that on cooling from 290 to 270 K, a CS interconversion occurs that is the opposite of the one that occurs on isothermal relaxation at 200 K. Second, in

this spectral region only minor changes in band position occur on cooling from 290 to 200 K. This is surprising because the influence of peak shift on vibrational bands is a well-known problem in variable temperature measurements (Nodland et al., 1996).

#### Comparison with single crystal spectrum and assignment to $B_I$ and $B_{II}$ substate

We next compare in Fig. 4 the single crystal spectrum of the  $\text{d}(\text{CGCGAATTCGCG})_2$  dodecamer (curve E, taken from

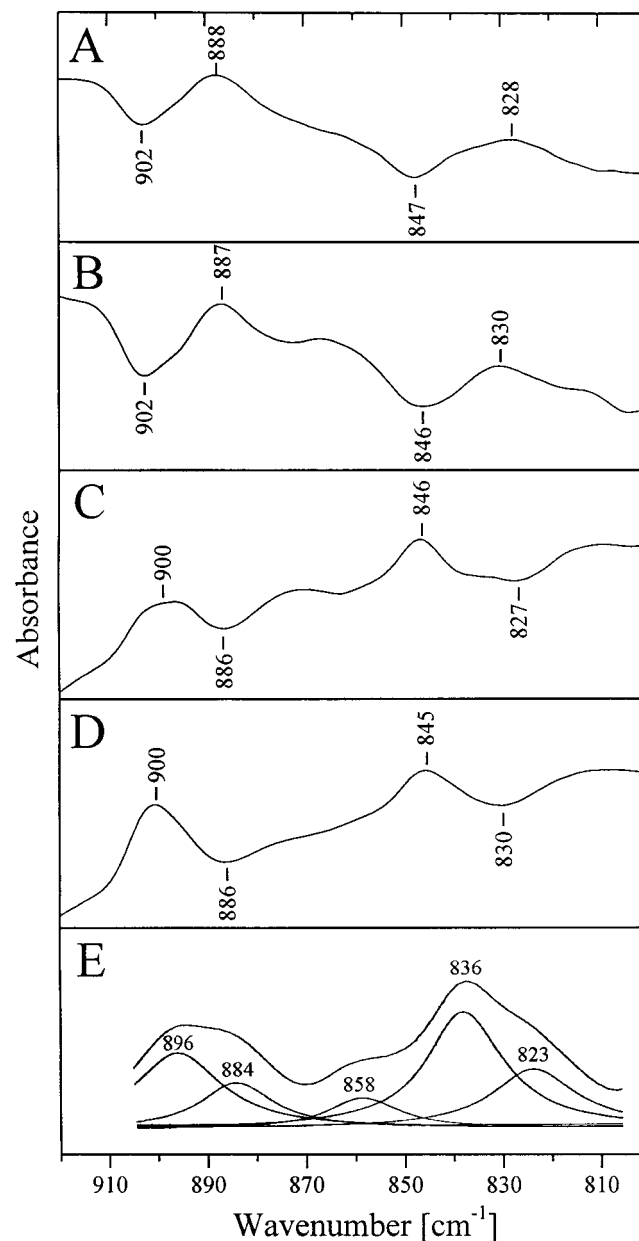


FIGURE 4 The comparison of difference curves obtained from unoriented hydrated films (A–D) with the spectrum of the single crystal of the  $\text{d}(\text{CGCGAATTCGCG})_2$  dodecamer (E). The curve resolved spectrum E was taken from Taillandier (1990) (see Fig. 3). The difference curves A–D are the same as those shown in Fig. 3, except that the range is restricted to 920–800  $\text{cm}^{-1}$ .

figure 3 of Taillandier, 1990), with the difference spectra obtained on isothermal relaxation at 200 K (*curves A and B*) and the 270–290 K difference spectra (*curves C and D*). Curves *A–D* are the same as shown in Fig. 3, but here the spectral range is shown only from 920 to 800  $\text{cm}^{-1}$  for the comparison with the single crystal spectrum. In curve *E* five component bands occur in the curve-resolved infrared spectrum of the single crystal, and the large variability in the sugar conformations, reflected by the existence of these component bands, has been pointed out before by Taillandier (1990). We surmise from our comparison that four of these single crystal component bands belong to two different CSs: the component bands centered at 896 and 836  $\text{cm}^{-1}$  have, at similar peak positions, negative features in the difference curves *A* and *B* and positive features in *C* and *D*, whereas for the component bands centered at 884 and 823  $\text{cm}^{-1}$  the opposite is observed. It follows that the component bands centered at 896 and 836  $\text{cm}^{-1}$  must belong to one CS in the single crystal, and the bands centered at 884 and 823  $\text{cm}^{-1}$  to another CS. The assignment of the component band centered at 858  $\text{cm}^{-1}$  is not clear, and in our experience the intensity of this band varies strongly with the type of baseline subtraction applied before curve resolution is attempted. The peak positions between the composite bands in *E* differ by several wavenumbers from those of the difference spectra from unoriented hydrated films shown from *A* to *D*. This is expected because differences of several wavenumbers are often observed when vibrational bands in a single crystal are compared with those in solution, for example, in the vibrational analysis of dimethyl and diethyl phosphates as model compounds for nucleic acids reported by Guan et al. (1994) and Guan and Thomas (1996a). Furthermore, peak positions can shift in difference spectra obtained from overlapping composite bands (Parry et al., 1991; Fleissner et al., 1995).

Because in the single crystal the  $B_I$ -to- $B_{II}$  population ratio is 10:1 (Fratini et al., 1982; Privé et al., 1987; Grzeskowiak et al., 1991), we assign in the single crystal spectrum the more intense bands centered at 896 and 836  $\text{cm}^{-1}$  to the  $B_I$  conformational substate and the less intense bands centered at 884 and 823  $\text{cm}^{-1}$  to the  $B_{II}$  substate. It seems obvious that on  $B_I$ -to- $B_{II}$  transition, the  $B_I$  band at 896  $\text{cm}^{-1}$  is converted into the  $B_{II}$  band at 884  $\text{cm}^{-1}$ , and the  $B_I$  band at 836  $\text{cm}^{-1}$  is converted into the  $B_{II}$  band at 823  $\text{cm}^{-1}$ . This assignment requires that for the pair of bands centered at 896 and 884  $\text{cm}^{-1}$ , the ratio of their molar extinction coefficients is 1:5.0, as the ratio of their relative band areas is 2.0:1. Similarly, for the pair of bands centered at 836 and 823  $\text{cm}^{-1}$ , the ratio of their molar extinction coefficients must be 1:5.5, as the ratio of their relative band areas is 1.8:1. A similar ratio of extinction coefficients has been observed before for band pairs of interconverting conformers, for example, for the axial and equatorial conformers of chlorocyclohexane (Fishman and Stolov, 1993). We consider the alternative assignment, i.e., 884  $\text{cm}^{-1}$  to  $B_I$  and 896  $\text{cm}^{-1}$  to  $B_{II}$ , less likely because the ratio of their molar extinction coefficients would have to be 1:20. We note that

these four bands can be used as marker bands for the  $B_I$  and  $B_{II}$  CS.

The  $B_I$ -to- $B_{II}$  transition involves not only the ionic phosphate, but also the sugar-phosphate backbone and the bases, and difference bands are observable in each of their characteristic spectral regions (see Figs. 1 and 2). Both the  $B_I$  and  $B_{II}$  substates generate a complete set of normal vibrations. For example, we have recently applied our method of isothermal relaxation in the glass→liquid transition region to chlorocyclohexane to separate the infrared spectra from its axial and equatorial conformer (Rüdiger et al., 1999). For both conformers a complete set of normal vibrations was obtained for the investigated spectral region. Depending on the spectral region, overlap between each of the normal vibrations of the axial and equatorial conformer varied greatly. In the same manner, two sets of normal vibrations are generated for both the  $B_I$  and  $B_{II}$  conformer substate, with greatly varying degrees of overlap between their normal modes.

The spectral region of Fig. 4 contains vibrations of the sugar-phosphate backbone and absorptions characteristic of the sugar pucker (Liquier and Taillandier, 1996). We attribute the decrease in wavenumber on  $B_I$ -to- $B_{II}$  transition observable in Fig. 4 (e.g., for Fig. 4 *A*: 902→888 and 847→828  $\text{cm}^{-1}$ ) to increased hydrogen bond interaction. This is consistent with our comparison of the spectral changes on  $B_I$ -to- $B_{II}$  transition with results from our recent MD simulation (Winger et al., 1998; see the Discussion). Further assignment of these two sets of bands to specific modes is not meaningful because, as pointed out by Guan and Thomas (1996a), significant coupling between the OPO ester modes and the modes of deoxyribose is expected. However, this does not preclude their use as marker bands for the  $B_I$  and  $B_{II}$  CS. For example, two marker bands of the axial conformer of chlorocyclohexane centered at 683 and 557  $\text{cm}^{-1}$  are widely used, although these bands are not well-localized C-Cl stretching vibrations, but are coupled with deformation and C-C stretching modes (Opaskar and Krimm, 1967).

It follows from the assignment given above that on isothermal relaxation of a quenched film at 200 K,  $B_I$  converts into  $B_{II}$ , whereas on cooling from 290 to 270 K (and lower, not shown),  $B_{II}$  converts into  $B_I$ . Similar temperature dependence has been reported for the CO conformer population in carbonylmyoglobin and attributed to the change in enthalpy and entropy with temperature (Hong et al., 1990).

### $B_I$ -to- $B_{II}$ conformer substate population ratio at 200 K

Curve resolution of infrared spectra of unoriented films of the dodecamer according to our method described recently (Fleissner et al., 1996) gives the population ratio of the  $B_I$ -to- $B_{II}$  conformer substates. We concentrate on the spectral region containing the symmetrical stretching vibration of the ionic phosphate,  $\nu_s$ , which is in the difference curve

of Fig. 1 at  $1084\text{ cm}^{-1}$  for  $B_I$  and at  $1099\text{ cm}^{-1}$  for  $B_{II}$ , because curve resolution of this spectral region turned out to be the most reliable one. Curve resolution of these bands requires a curve fit containing the overlapping band region from  $1155$  to  $995\text{ cm}^{-1}$ . Fig. 5 A shows the experimental composite band of the spectrum recorded at  $200\text{ K}$  after  $4\text{ min}$  (solid line, two-point baseline corrected), the eight curve-fitted component bands that were necessary to optimize the curve fit, and their sum (dashed line), which is indistinguishable from the experimental composite band. Six of the component bands are seen already in the experimental composite band in the form of peaks or shoulders. In Fig. 5 B the second derivative of the experimental composite band (solid line) shows these six component bands as distinct peaks. The seventh and eighth component bands were necessary to reproduce the asymmetry at  $\sim 1091\text{ cm}^{-1}$  in the second derivative and the weak feature at  $1033\text{ cm}^{-1}$ . The fourth derivative curve has distinct weak peaks at these positions (not shown).

The degree of overlap in composite band profiles is characterized by a parameter  $\delta$ , which is defined as

$$\delta = \nu_2 - \nu_1(1/\text{FWHH}_1 + 1/\text{FWHH}_2) \quad (1)$$

where  $\nu_1$  and  $\nu_2$  are the peak maxima of two overlapping bands, and  $\text{FWHH}_1$  and  $\text{FWHH}_2$  are their full widths at half-height (Vandeginste and De Galan, 1975; Maddams, 1980). As a general rule, reliable curve fitting of two overlapping bands of unknown band shape is possible only for  $\delta > 2$ , i.e., when separation of their peak maxima is larger than their average FWHH. This even holds when the number of bands is known. We have recently shown that curve fitting of highly overlapping bands can be improved by comparison of the second or fourth derivative of the experimental composite band profile with that of the sum of the curve-fitted component bands (Fleissner et al., 1996). Optimization is achieved with fixed values of one or more band parameters, aiming thereby for optimal correspondence between the derivative curves. With this additional criterion it was possible to resolve reliably overlapping bands into their component bands with  $\delta$  as low as  $0.7$ , i.e., separation of two bands by only about a third of their average FWHH can, in favorable cases, be sufficient for reliable curve resolution. This method requires data with very high signal-to-noise ratios, which are easily obtained with FT-IR spectrometers. This comparison of derivative curves is, in our

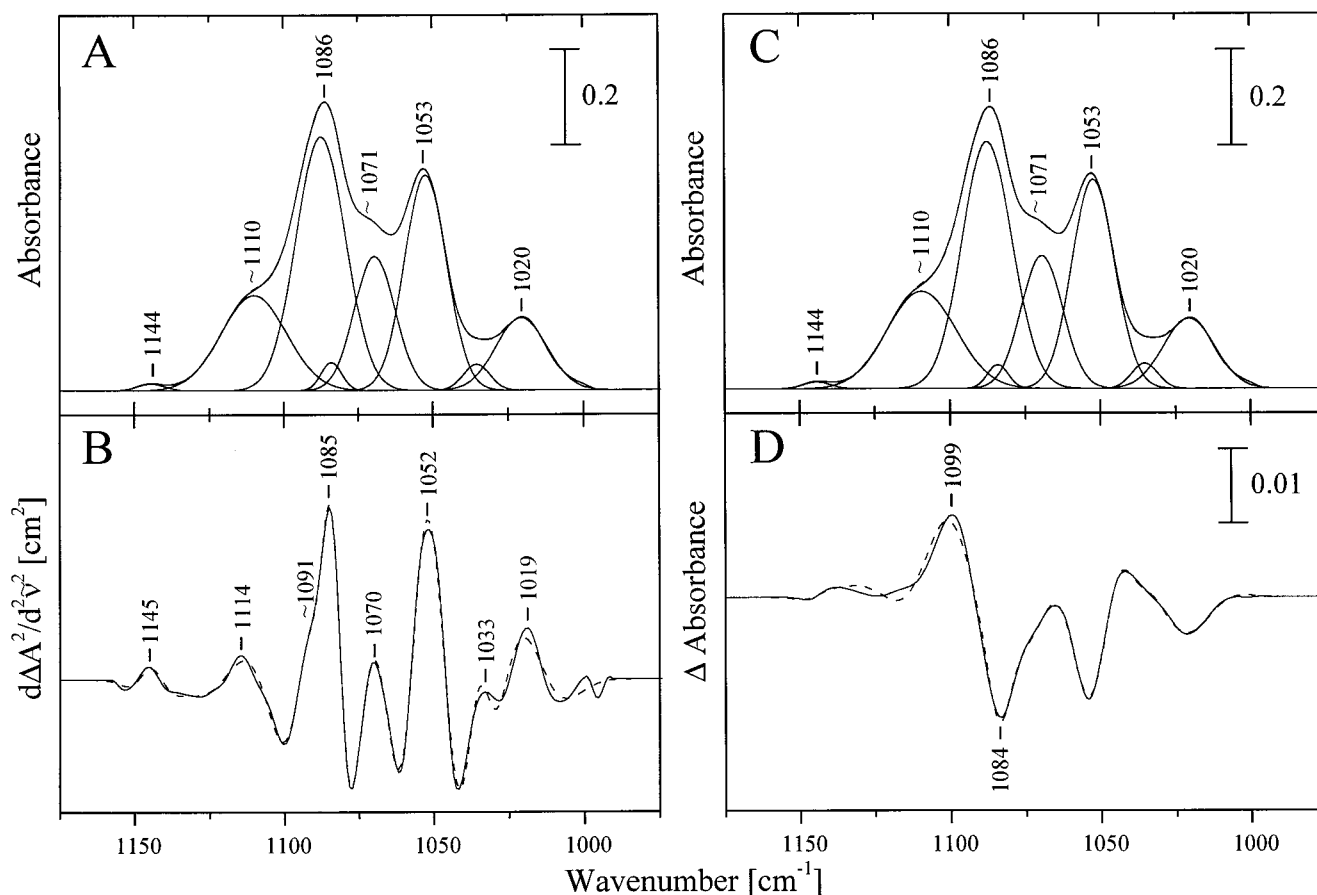


FIGURE 5 Curve resolution of spectra of the unoriented  $d(\text{CGCGAATTCGCG})_2$  dodecamer film recorded at  $200\text{ K}$  ( $\Gamma = 13$ , from  $1175$  to  $975\text{ cm}^{-1}$ ). (A) The experimental composite spectrum recorded at  $200\text{ K}$  after  $4\text{ min}$  (—), the eight curve-fitted component bands, and their sum (---). (B) The comparison of the second derivative curve of the experimental composite band profile (—) with that of the sum of the curve-fitted component bands (---). (C) The experimental composite spectrum recorded at  $200\text{ K}$  after  $25\text{ min}$  (—), the eight curve-fitted component bands, and their sum (---). (D) The comparison of the experimental difference curve (—,  $C - A$ ) with that of the sum of the curve-fitted component bands (---,  $C - A$ ).

experience, superior to using (reduced)  $\chi^2$  values as parameters for goodness of fit.

Fig. 5 B shows such a comparison between the second derivative of the experimental composite band (*solid line*) and the sum of the curve-fitted component bands from Fig. 5 A (*dashed line*). In this fortunate case, optimal correspondence was achieved without fixing any band parameters in the beginning of the fit. In the next step the isothermal changes on relaxation by interconversion of the two conformers were quantified by curve-fitting an experimental composite band obtained from a spectrum recorded at 200 K after 25 min (Fig. 5 C). Band parameters of the curve fit shown in Fig. 5 A were used as starting parameters. This experimental composite band, the eight component bands, and their sum are shown in Fig. 5 C. In a third step further minor refinement of the curve fit was achieved by comparison of the difference curve obtained by subtracting the baseline-corrected experimental composite band recorded after 25 min from that after 4 min (Fig. 5 D, *solid line*), with the difference curve obtained from the sum of the two curve fits (Fig. 5 D, *dashed line*,  $C - A$ ). This optimization is, in our experience, a very useful additional criterion for the quality of the curve fits. The band parameters of both curve fits optimized as described are listed in Table 1. This optimization required for Fig. 5 C to fix the peak maximum and FWHH of the two component bands centered at 1087.4 and 1084.0  $\text{cm}^{-1}$ . The number of significant digits was chosen in such a way that the change in band area of the band centered at 1144  $\text{cm}^{-1}$  gives the experimentally observed negative feature in the difference spectrum of Fig. 5 D.

The component band centered at 1109  $\text{cm}^{-1}$  is much broader than that at 1087  $\text{cm}^{-1}$  (Table 1, 26 versus 19  $\text{cm}^{-1}$ ). Koenig (1992) pointed out that “the amplitude of the

peaks in derivative spectra are a function of the widths of the original peaks, and this condition leads to a heavy bias toward the sharper peaks present in the original spectra.” Because of this, the broad band at 1109  $\text{cm}^{-1}$  is only a weak feature in the second derivative curve in comparison to the peak at 1085  $\text{cm}^{-1}$  (Fig. 5 B). For the same reason, we preferred the comparison of second derivative curves, instead of fourth derivatives (Fleissner et al., 1996), because in the latter case the broad band is barely recognizable.

Changes in areas of the two component bands centered at 1087 and 1109  $\text{cm}^{-1}$  (assigned above to  $\nu_s$  of the ionic phosphate in B<sub>I</sub> and B<sub>II</sub>) on conformer interconversion from 4 to 25 min are used in our following estimation of the conformer substate population ratio, because these curve-fitted component bands, with a  $\delta$  value of 2.0, are the most reliable ones. The band area ratio of these two bands is 2.02:1 for the curve fit of Fig. 5 A (read from Table 1). The ratio of their extinction coefficients is obtained by comparison with the curve fit of Fig. 5 C. The area of the component band centered at 1087  $\text{cm}^{-1}$  decreases by 2.62%, whereas the area of the component band centered at 1109  $\text{cm}^{-1}$  increases by 3.15% (of the band centered at 1087  $\text{cm}^{-1}$ ). Therefore, the ratio of extinction coefficients,  $J_{(1087)}/J_{(1109)}$ , is 0.831. From these values we calculate our estimation of the conformer substate population ratio after 4 min at 200 K (Fig. 5 A) as 2.4:1 for the disappearing and formed CS, i.e., for B<sub>I</sub> and B<sub>II</sub>, and, after 25 min, as 2.2:1.

As a further test, the same procedure was applied to the experimental composite profile of a spectrum recorded after 10 and after 63 min, and the conformer population ratio was determined by comparison with the spectrum recorded after 4 min (Fig. 5 A). Estimation of the B<sub>I</sub>-to-B<sub>II</sub> population ratio gave 2.3:1 and 2.1:1. We thus estimate the B<sub>I</sub>-to-B<sub>II</sub> substate population ratio as  $2.4 \pm 0.5$ :1 for the spectrum recorded at 200 K after 4 min.

**TABLE 1** Curve-fitting analysis of the infrared spectra (from 1175 to 975  $\text{cm}^{-1}$ ) of a quenched d(CGCGAATTCGCG)<sub>2</sub> dodecamer film, with  $\Gamma = 13$ , recorded at 200 K after 4 min and 25 min

Band no.		$\nu_{\text{max}}$ ( $\text{cm}^{-1}$ )	Height	FWHH ( $\text{cm}^{-1}$ )	Area
1	4 min	1144.4	0.0142	10.8	0.164
	25 min	1144.2	0.0141	10.8	0.163
2	4 min	1109.9	0.1969	25.7	5.384
	25 min	1109.2	0.2012	26.7	5.727
3	4 min	1087.4	0.5258	19.4	10.870
	25 min	1087.4	0.5121	19.4	10.585
4	4 min	1084.0	0.0582	8.0	0.497
	25 min	1084.0	0.0493	8.0	0.420
5	4 min	1069.4	0.2776	16.1	4.748
	25 min	1069.3	0.2757	16.1	4.729
6	4 min	1052.3	0.4465	16.4	7.778
	25 min	1052.2	0.4337	16.6	7.676
7	4 min	1035.4	0.0541	10.3	0.594
	25 min	1035.2	0.0528	10.2	0.572
8	4 min	1020.5	0.1500	19.9	3.169
	25 min	1020.4	0.1451	20.0	3.092

For Tables 1 and 2:  $\nu_{\text{max}}$  (in  $\text{cm}^{-1}$ ) are the peak frequencies; FWHH is the full width at half-height of the curve-fitted component bands.

### B<sub>I</sub>-to-B<sub>II</sub> conformer substate population ratio at ambient temperature

The B<sub>I</sub>-to-B<sub>II</sub> conformer substate population ratio at ambient temperature was estimated in the same manner. Fig. 6 A shows the experimental composite band of the spectrum recorded at 290 K (*solid line*,  $\Gamma = 13$ , two-point baseline corrected), the same eight curve-fitted component bands used for the curve fit at 200 K, and their sum (*dashed line*). In Fig. 6 B the second derivative of the experimental composite band (*solid line*) is compared with the sum of the curve-fitted component bands (*dashed line*). Fig. 6 C shows the experimental composite of the spectrum recorded at 270 K (*solid line*), the eight curve-fitted component bands, and their sum (*dashed line*, almost congruent with the *solid line*). In Fig. 6 D the experimental difference curve obtained by subtracting the baseline-corrected experimental spectrum recorded at 290 K from that at 270 K (*solid line*) is compared with the difference curve obtained from the sum of the corresponding curve fits (*dashed line*,  $C - A$ ). The band

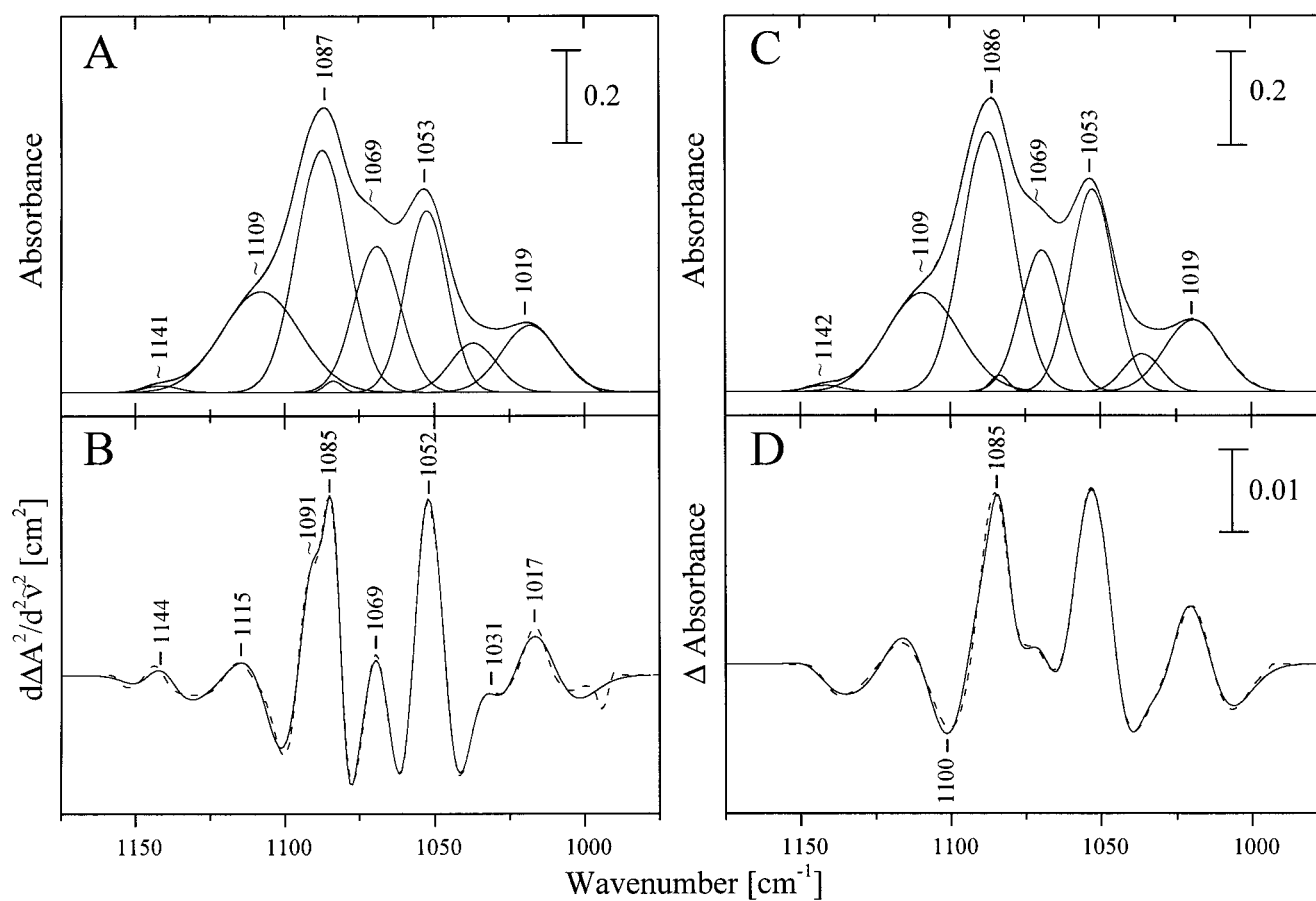


FIGURE 6 Curve resolution of spectra of the unoriented  $d(CGCGAATTCGCG)_2$  dodecamer film recorded at 290 and 270 K ( $\Gamma = 14$ , from 1175 to 975  $\text{cm}^{-1}$ ). (A) The experimental composite spectrum recorded at 290 K (—), the eight curve-fitted component bands, and their sum (---). (B) The comparison of the second derivative curve of the experimental composite band profile (—) with that of the sum of the curve-fitted component bands (---). (C) The experimental composite spectrum recorded at 270 K (—), the eight curve-fitted component bands, and their sum (---). (D) The comparison of the experimental difference curve (—,  $C - A$ ) with that of the sum of the curve-fitted component bands (---,  $C - A$ ).

parameters of both curve fits optimized as described above are listed in Table 2.

The band area ratio of the two bands centered at 1087 and 1108  $\text{cm}^{-1}$  is 1.58:1. The area of the component band centered at 1087  $\text{cm}^{-1}$  increases on cooling to 270 K by 7.15%, whereas the area of the component band centered at 1108  $\text{cm}^{-1}$  decreases by 5.48% (of the band centered at 1087  $\text{cm}^{-1}$ ). Therefore, the ratio of extinction coefficients,  $J_{(1087)}/J_{(1108)}$ , is 1.31. From these values we calculate our estimation of the  $B_I$ -to- $B_{II}$  substate conformer population ratio as 1.2:1 for 290 K and as 1.4:1 for 270 K. This change in CS population is consistent with interconversion of  $B_{II}$  into  $B_I$  on cooling from ambient temperature. Further curve fits of spectra recorded at 280 and 260 K are consistent with this estimation (not shown). From these curve fits and the two curve fits shown above, our estimation for the  $B_I$ -to- $B_{II}$  population ratio is  $1.3 \pm 0.5$ :1 for the temperature range 270–290 K. These values are for equilibrated samples, because at these temperatures the rate of CS interconversion is very high (Hogan and Jardetzky, 1979; Chou et al., 1992; Gorenstein, 1994). This is consistent with our experience that at temperatures greater than or equal to 260 K, differ-

ence curves obtained isothermally at a given temperature contain only noise. One assumption in our estimation is that the ratio of extinction coefficients is constant. We expect the error to be minor because the temperature range used for the estimation is small.

## DISCUSSION

### Spectroscopic features of water migration

Our discussion of the difference curves (Fig. 2) concentrates on the following three spectral regions: 1) the OH stretching band region of water from 4000 to 2000  $\text{cm}^{-1}$ ; 2) the region containing the  $\text{H}_2\text{O}$  bending vibration at  $\sim 1660 \text{ cm}^{-1}$ , stretching vibrations of double bonds in the base planes and bands due to the base-sugar entities (from 1800 to 1350  $\text{cm}^{-1}$ ); and 3) the region containing absorptions of the ionic phosphate groups and of the sugar and vibrations of the phosphodiester backbone coupled to the vibrations of the sugar (from 1350 to 800  $\text{cm}^{-1}$ ) (Parker, 1983; Taillandier and Liquier, 1992; Cao et al., 1995; Liquier and Taillandier, 1996; Guan and Thomas, Jr., 1996a). Pronounced spectral

**TABLE 2** Curve-fitting analysis of the infrared spectra (from 1175 to 975 cm<sup>-1</sup>) of a quenched d(CGCGAATTCGCG)<sub>2</sub> dodecamer film, with  $\Gamma = 13$ , recorded at 290 K and 270 K

Band no.		$\nu_{\max}$ (cm <sup>-1</sup> )	Height	FWHH (cm <sup>-1</sup> )	Area
1	290 K	1141.4	0.0141	13.7	0.206
	270 K	1141.8	0.0134	14.0	0.200
2	290 K	1107.9	0.2133	30.7	6.973
	270 K	1109.2	0.2095	28.6	6.368
3	290 K	1087.3	0.5138	20.2	11.048
	270 K	1087.3	0.5505	20.2	11.838
4	290 K	1083.7	0.0244	6.8	0.177
	270 K	1083.7	0.0349	6.8	0.253
5	290 K	1068.9	0.3093	18.0	5.934
	270 K	1069.3	0.2998	16.8	5.353
6	290 K	1052.4	0.3849	16.2	6.621
	270 K	1052.5	0.4291	16.8	7.667
7	290 K	1036.9	0.1041	18.1	2.001
	270 K	1036.1	0.0803	14.4	1.234
8	290 K	1018.0	0.1409	22.2	3.327
	270 K	1019.2	0.1518	22.3	3.612

changes on B<sub>I</sub>-to-B<sub>II</sub> interconversion occur for the intense bands in the antisymmetrical and symmetrical stretching band region of the PO<sub>2</sub><sup>-</sup> group (see Fig. 2, 1208→1236 and 1209→1243 cm<sup>-1</sup>, 1083→1100 and 1085→1101 cm<sup>-1</sup>). The increase in frequency in going from B<sub>I</sub> to B<sub>II</sub> is attributed to increasing bond strength caused by a decrease in hydrogen-bond interaction with water molecules (Pohle et al., 1990; Guan and Thomas, 1996b). Phosphodiester backbone and sugar moiety vibrations (from 1300 to 800 cm<sup>-1</sup>) are shifted to lower frequency on B<sub>I</sub>-to-B<sub>II</sub> interconversion (for example, see Fig. 2, bottom: 976→959, 903→886, 847→829 cm<sup>-1</sup>), which is attributed to increasing hydrogen-bond interaction. Simultaneous changes in water's OH-stretching band region are consistent with increasing hydrogen-bond interaction on B<sub>I</sub>-to-B<sub>II</sub> transition (see Figs. 1 and 2), as two negative peaks at ~3490 and ~3285 cm<sup>-1</sup> indicate weak hydrogen-bond interaction in B<sub>I</sub>, and the broad positive peak centered at ~2840 cm<sup>-1</sup> indicates increased hydrogen-bond interaction in B<sub>II</sub>. In the corresponding spectral region of B-DNA from salmon testes, a negative peak is centered at ~3240 cm<sup>-1</sup>, and a shoulder is observable at ~3480 cm<sup>-1</sup> (Fig. 2, bottom), similar to the frequencies of the dodecamer. A broad positive peak at lower frequency is barely observable. This is attributed to a much wider distribution of OH oscillators in highly polymeric B-DNA than for the dodecamer. The above-mentioned three types of spectral changes in going from B<sub>I</sub> to B<sub>II</sub> seem to happen in concert. They are consistent with migration of weakly hydrogen-bonded water from the ionic phosphate in B<sub>I</sub> toward the oxygens of the phosphodiester and/or sugar moieties in B<sub>II</sub>. This interpretation of the experimentally observed spectroscopic changes is consistent with our recent MD simulation and the analysis of the B<sub>I</sub>-to-B<sub>II</sub> interconversion (Winger et al., 1998).

B<sub>I</sub>-to-B<sub>II</sub> interconversion also involves the bases, as can be seen in the spectral region containing the in-plane double

bond stretching vibrations. This region is partly obscured by the intense deformation mode of water, but second derivative curves still allow us to observe these spectral changes (not shown). In this spectral region minor spectroscopic differences between the difference spectra of the dodecamer and that of B-DNA from salmon testes result from the different base pair population, because GC content is 66% in the dodecamer and 41% in DNA from salmon testes (Chagraff et al., 1951). We therefore only concentrate on the pronounced spectral change on B<sub>I</sub>-to-B<sub>II</sub> interconversion from 1719 to 1707 cm<sup>-1</sup> in the dodecamer (from 1720 to 1711 cm<sup>-1</sup> for B-DNA from salmon testes, Fig. 2). This infrared band is assigned mainly to the C=O and C=N stretching vibrations of the bases. This spectral region is extremely sensitive to base stacking, and similar low-frequency shift on transition of B-DNA to A-DNA has been attributed to changes in base stacking (Taillandier and Liquier, 1992; Cao et al., 1995; Liquier and Taillandier, 1996). The same interpretation is reasonable for the spectral change on B<sub>I</sub>-to-B<sub>II</sub> transition. Spectral changes of the base vibrations occur on time scales similar to those of the ionic phosphate and phosphodiester sugar backbone moieties (Rüdiger et al., 1997b).

### Consequences of enhanced B<sub>II</sub> substate population for induced-fit-type dynamics of the protein recognition process

The biological consequences of B<sub>I</sub> and B<sub>II</sub> substates have been discussed before with respect to protein-DNA interaction (Fratini et al., 1982; Gorenstein, 1994) and the rates of spontaneous transition mutations (Mitra et al., 1995). Here we concentrate on the biological significance of our quantification of B<sub>II</sub> substate population in unoriented films of naturally occurring B-DNA and the dodecamer, and the coupling of water migration with base destacking.

The similarity of difference spectra of highly polymeric B-DNA and the dodecamer (Fig. 2) proves that the internal dynamics of B-DNA probed by low-temperature relaxation must be localized. Therefore information derived from oligonucleotides gives insight into the structure and dynamics of B-DNA of high molecular weight.

It has been suggested that the appearance of the B<sub>II</sub> substate in single-crystal x-ray studies might be linked to crystal packing effects (Dickerson et al., 1987). The opposite seems to be true for the Drew-Dickerson dodecamer, and crystal packing effects apparently can suppress the B<sub>II</sub> substate. This B<sub>II</sub> population difference between unoriented and crystalline dodecamer is not caused by differences in hydration, as hydration in the single crystal is similar to that of the two investigated unoriented dodecamer films ( $\Gamma = 13$  and 14, versus  $\Gamma \approx 18$  in the crystal; Kopka et al., 1983). Because this hydration range is the one found, for example, in chromatin (Garner and Burg, 1994), a high B<sub>II</sub> substate population is expected in vivo.

The effect of base pair length on B<sub>II</sub> substate population seems to be minor in the unoriented films. It has been

pointed out that end effects influence the oligomer structures, and crystal packing has significant effects on the local geometry of the helical fragments in oligomers (Chandrasekaran and Arnott, 1996). Because in the crystalline dodecamer B<sub>II</sub> occurs only at the end positions (at G10 and G22), it could be caused by crystal packing effects (Dickerson et al., 1987). But in unoriented films of the dodecamer, the B<sub>II</sub> population is much higher than in the crystal; therefore B<sub>II</sub> must also occur toward the middle. For B-DNA from salmon testes, with lengths between ~400 and >5000 bp, end effects are negligible.

Grzeskowiak et al. (1991) pointed out that "destacking of two successive bases along one chain is a necessary but not sufficient condition for adoption of B<sub>II</sub> phosphate conformation," and inquire, "what additional factors decide whether the phosphate will slip into the B<sub>II</sub> conformation or not?" We propose that migration of water from ionic phosphate toward the oxygens of the phosphodiester or sugar moiety or both is necessary for interconversion from B<sub>I</sub> to B<sub>II</sub>, in addition to destacking of bases. This requires that water exchange is coupled to the conformational B<sub>I</sub>-to-B<sub>II</sub> transition. In this scheme, the B<sub>II</sub> substate is stabilized in comparison to B<sub>I</sub> by enhanced hydrogen-bond interaction on migration of water from ionic phosphate to the oxygens of the phosphodiester or sugar moieties (see Fig. 2, minima at ~3490 and ~3285 cm<sup>-1</sup> for B<sub>I</sub> and maximum at ~2840 cm<sup>-1</sup> for B<sub>II</sub>). At first this seems to contradict experimental studies in which hydrogen-bonding of water to ionic phosphate is strong (Falk et al., 1962a), but this holds for the first two water molecules only. Additional water molecules could be much more weakly hydrogen-bonded. Unspecific interaction of proteins with B-DNA could generate the B<sub>II</sub> substate in a similar manner by hydrogen-bond interaction with the oxygens of the phosphodiester or the sugar (Pabo and Sauer, 1992; Travers, 1994; Luisi, 1995).

The bases are also involved in the B<sub>I</sub>-to-B<sub>II</sub> interconversion because spectroscopic changes occur not only for vibrations of the phosphate/sugar backbone, but also for those of the bases. Because these spectroscopic changes occur on time scales similar to those of the sugar-phosphate backbone (Rüdiger et al., 1997b), the conformational changes are coupled. It is most likely the two successive bases along one chain with the phosphate in between are involved in the B<sub>I</sub>-to-B<sub>II</sub> interconversion. Therefore, nonspecific interaction of a protein with DNA at the phosphate backbone could become specific once the B<sub>I</sub> and B<sub>II</sub> substates and their conformational coupling with the bases are considered.

Coupling of base destacking with water migration from ionic phosphate to the sugar oxygen on B<sub>I</sub>-to-B<sub>II</sub> transition was also observed in our recent molecular dynamics simulation of the d(CGCGAATTCGCG)<sub>2</sub> dodecamer (Winger et al., 1998). This simulation further showed that on B<sub>I</sub>-to-B<sub>II</sub> transition, comparatively slow base destacking occurs first, which then can be followed by very fast change of the backbone conformation and migration of water. In this highly dynamic system, which fluctuates between the B<sub>I</sub> and B<sub>II</sub> substates, a protein approaching B-DNA can select

the B<sub>I</sub> or B<sub>II</sub> substate, depending on which one gives optimal interaction with the bases and the sugar-phosphate backbone.

We propose that nonspecific interaction of proteins with the DNA backbone could become specific by induced-fit-type contact with backbone in either B<sub>I</sub> or B<sub>II</sub> conformation, because adoption of the CSs apparently also depends on base sequence (Grzeskowiak et al., 1991). One example is the report by Otwinowski et al. (1988) on the crystal structure of the trp repressor/operator complex: there are no direct hydrogen bonds to the bases, and the base sequence seems to be recognized indirectly through its effects on the geometry of the phosphate backbone. Consideration of the B<sub>I</sub> or B<sub>II</sub> CSs and their relation to base sequence could help explain these findings. Resolution of x-ray structures of protein-DNA complexes is at present not sufficient to detect these backbone CSs; but they can be studied by NMR (Szyperski et al., 1997) and vibrational spectroscopy.

We are grateful to Prof. Taillander for information and to the "Forschungsförderungsfonds" of Austria for financial support (project P12319-PHY).

## REFERENCES

- Arnott, S., P. J. Campbell Smith, and R. Chandrasekaran. 1975. CRC Handbook of Biochemistry and Molecular Biology, Vol. 2, Nucleic Acids. CRC Press, Cleveland, OH. 411–422.
- Cao, A., J. Liquier, and E. Taillander. 1995. Infrared and Raman spectroscopy of biomolecules. In *Infrared and Raman Spectroscopy*. B. Schrader, editor. VCH, Weinheim. 344–355.
- Chargaff, E., R. Lipshitz, Ch. Green, and M. E. Hodes. 1951. The composition of the desoxyribonucleic acid of salmon sperm. *J. Biol. Chem.* 192:223–230.
- Chandrasekaran, R., and S. Arnott. 1996. The structure of B-DNA in oriented fibers. *J. Biomol. Struct. Dyn.* 13:1015–1027.
- Chou, S.-H., J.-W. Cheng, and B. R. Reid. 1992. Solution structure of [d(ATGAGCGAATA)]<sub>2</sub>. *J. Mol. Biol.* 228:138–155.
- Cruse, W. B. T., S. A. Salisbury, T. Brown, R. Cosstick, F. Eckstein, and O. Kennard. 1986. Chiral phosphorothioate analogues of B-DNA. *J. Mol. Biol.* 192:891–905.
- Dickerson, R. E., D. S. Goodsell, M. L. Kopka, and P. E. Pjura. 1987. The effect of crystal packing on oligonucleotide double helix structure. *J. Biomol. Struct. Dyn.* 5:557–579.
- Falk, M., K. A. Hartman, Jr., and R. C. Lord. 1962a. Hydration of deoxyribonucleic acid. I. A gravimetric study. *J. Am. Chem. Soc.* 84: 3843–3846.
- Falk, M., K. A. Hartman, Jr., and R. C. Lord. 1962b. Hydration of deoxyribonucleic acid. II. An infrared study. *J. Am. Chem. Soc.* 84: 3843–3846.
- Falk, M., A. G. Poole, and C. G. Goymour. 1970. Infrared study of the state of water in the hydration shell of DNA. *Can. J. Chem.* 48:1536–1542.
- Fishman, A. I., and A. A. Stolov. 1993. Vibrational spectroscopic approaches to conformational equilibria and kinetics (in condensed media). *Spectrochim. Acta.* 49A:1435–1479.
- Fleissner, G., A. Hallbrucker, and E. Mayer. 1995. Ion-pairing as indicator for enhanced mobility in the glassy state of hyperquenched solution. *J. Phys. Chem.* 99:8401–8404.
- Fleissner, G., W. Hage, A. Hallbrucker, and E. Mayer. 1996. Improved curve resolution of highly overlapping bands by comparison of fourth-derivative curves. *Appl. Spectrosc.* 50:1235–1245.
- Fleissner, G., A. Hallbrucker, and E. Mayer. 1998. Increasing contact-ion pairing as a supercooled water anomaly. Estimation of the fictive temperature of hyperquenched glassy water. *J. Phys. Chem.* 102: 6239–6247.

- Fratini, A. V., M. L. Kopka, H. R. Drew, and R. E. Dickerson. 1982. Reversible bending and helix geometry in a B-DNA dodecamer: CGC-GAATT<sup>Br</sup>CGCG. *J. Biol. Chem.* 257:14686–14707.
- Garner, M. M., and M. B. Burg. 1994. Macromolecular crowding and confinement in cells exposed to hypertonicity. *Am. J. Physiol.* 266: C877–C892.
- Gorenstein, D. G. 1994. Conformation and dynamics of DNA and protein-DNA complexes by <sup>31</sup>P NMR. *Chem. Rev.* 94:1315–1338.
- Grzeskowiak, K., K. Yanagi, G. G. Privé, and R. E. Dickerson. 1991. The structure of B-helical C-G-A-T-C-G-A-T-C-G and comparison with C-C-A-A-C-G-T-T-G-G. *J. Biol. Chem.* 266:8861–8883.
- Guan, Y., Ch. J. Wurrey, and G. J. Thomas, Jr. 1994. Vibrational analysis of nucleic acids. I. The phosphodiester group in dimethyl phosphate model compounds: (CH<sub>3</sub>O)<sub>2</sub>PO<sub>2</sub><sup>−</sup>, (CD<sub>3</sub>O)<sub>2</sub>PO<sub>2</sub><sup>−</sup>, and (<sup>13</sup>CH<sub>3</sub>O)<sub>2</sub>PO<sub>2</sub><sup>−</sup>. *Biophys. J.* 66:225–235.
- Guan, Y., and G. J. Thomas, Jr. 1996a. Vibrational analysis of nucleic acids. IV. Normal modes of the DNA phosphodiester structure modeled by diethyl phosphate. *Biopolymers.* 39:813–835.
- Guan, Y., and G. J. Thomas, Jr. 1996b. Vibrational analysis of nucleic acids. III. Conformation-dependent Raman markers of the phosphodiester backbone modeled by dimethyl phosphate. *J. Mol. Struct.* 379: 31–41.
- Hogan, M. E., and O. Jardetzky. 1979. Internal motions in DNA. *Proc. Natl. Acad. Sci. USA.* 76:6341–6345.
- Hong, M. K., D. Braunstein, B. R. Cowen, H. Frauenfelder, I. E. T. Iben, J. R. Mourant, P. Ormos, R. Scholl, A. Schulte, P. J. Steinbach, A.-H. Xie, and R. D. Young. 1990. Conformational substates and motions in myoglobin. *Biophys. J.* 58:429–436.
- Huber, Ch. G., P. J. Oefner, and G. K. Bonn. 1995. Rapid and accurate sizing of DNA fragments by ion-pair chromatography on alkylated nonporous poly(styrene-divinylbenzene) particles. *Anal. Chem.* 67: 578–585.
- Koenig, J. L. 1992. Spectroscopy of Polymers. American Chemical Society, Washington, DC. 62.
- Kopka, M. L., A. V. Fratini, H. R. Drew, and R. E. Dickerson. 1983. Ordered water structure around a B-DNA dodecamer. A quantitative study. *J. Mol. Biol.* 163:129–146.
- Kubasek, W. L., Y. Wang, G. A. Thomas, Th. W. Patapoff, K.-H. Schoenwaelder, J. H. Van der Sande, and W. L. Peticolas. 1986. Raman spectra of the model B-DNA oligomer d(CGCGAATTCGCG)<sub>2</sub> and of the DNA in living salmon sperm show that both have very similar B-type conformations. *Biochemistry.* 25:7440–7445.
- Liquier, J., and E. Taillandier. 1996. Infrared spectroscopy of nucleic acids. In *Infrared Spectroscopy of Biomolecules*. H. H. Mantsch and D. Chapman, editors. Wiley-Liss, New York. 131–158.
- Luisi, B. 1995. DNA-protein interaction at high resolution. In *DNA-Protein: Structural Interactions*. D. M. J. Lilley, editor. IRL Press, Oxford. 1–48.
- Maddams, W. F. 1980. The scope and limitations of curve fitting [to vibrational band systems]. *Appl. Spectrosc.* 32:245–267.
- Mitra, R., B. M. Pettitt, and R. D. Blake. 1995. Conformational states governing the rates of spontaneous transition mutations. *Biopolymers.* 36:169–179.
- Nodland, E., F. O. Libnau, O. M. Kvalheim, H.-J. Luinge, and P. Klæboe. 1996. Influence and correction of peak shift and band broadening observed by rank analysis on vibrational bands from variable-temperature measurements. *Vibrational Spectrosc.* 10:105–123.
- Opaskar, C. G., and S. Krimm. 1967. A force field for secondary chlorides. *Spectrochim. Acta.* 23A:2261–2278.
- Otwinowski, Z., R. W. Schevitz, R.-G. Zhang, C. L. Lawson, A. Joachimiak, R. Q. Marmorstein, B. F. Luisi, and P. B. Sigler. 1988. Crystal structure of trp repressor/operator complex at atomic resolution. *Nature.* 335:321–329.
- Pabo, C. O., and R. T. Sauer. 1992. Transcription factors: structural families and principles of DNA recognition. *Annu. Rev. Biochem.* 61: 1053–1095.
- Parker, F. S. 1983. Applications of Infrared, Raman, and Resonance Raman Spectroscopy in Biochemistry. Plenum Press, New York. 349–398.
- Parry, D. B., M. G. Samant, and O. R. Melroy. 1991. Interpreting IR difference spectra. *Appl. Spectrosc.* 45:999–1007.
- Peticolas, W. L. 1995. Raman spectroscopy of DNA and proteins. *Methods Enzymol.* 246:389–416.
- Pohle, W., M. Bohl, and H. Böhlig. 1990. Interpretation of the influence of hydrogen bonding on the stretching vibrations of the PO<sub>2</sub><sup>−</sup> moiety. *J. Mol. Struct.* 242:333–342.
- Privé, G. G., U. Heinemann, S. Chandrasekaran, L.-S. Kan, M. L. Kopka, and R. E. Dickerson. 1987. Helix geometry, hydration and G.A mismatch in a B-DNA decamer. *Science.* 238:498–504.
- Rüdissler, S. 1997. Ph.D. thesis. University of Innsbruck.
- Rüdissler, S., G. Fleissner, A. Pichler, A. Hallbrucker, and E. Mayer. 1999. Separation of chlorocyclohexane's axial and equatorial conformer infrared spectrum by isothermal relaxation in the glass→liquid transition region. *J. Mol. Struct.* 479:237–243.
- Rüdissler, S., A. Hallbrucker, and E. Mayer. 1996. Probing DNA's dynamics and conformational substates by enthalpy relaxation and its recovery. *J. Phys. Chem.* 100:458–461.
- Rüdissler, S., A. Hallbrucker, E. Mayer, and G. P. Johari. 1997a. Enthalpy, entropy, and structural relaxation behaviors of A- and B-DNA in their vitrified states and the effect of water on the dynamics of B-DNA. *J. Phys. Chem.* 101:266–277.
- Rüdissler, S., A. Hallbrucker, and E. Mayer. 1997b. B-DNA's conformational substates revealed by Fourier transform infrared difference spectroscopy. *J. Am. Chem. Soc.* 119:12251–12256.
- Saareinen, P. E., J. K. Kauppinen, and J. O. Partanen. 1995. New method for spectral line shape fitting and critique on the Voigt line shape model. *Appl. Spectrosc.* 49:1438–1453.
- Seshadri, K. S., and R. N. Jones. 1963. The shapes and intensities of infrared absorption bands—a review. *Spectrochim. Acta.* 19:1013–1085.
- Song, Z., O. N. Antzutkin, Y. K. Lee, S. C. Shekar, A. Rupprecht, and M. H. Levitt. 1997. Conformational transitions of the phosphodiester backbone in native DNA: two-dimensional magic-angle-spinning <sup>31</sup>P-NMR of DNA fibers. *Biophys. J.* 73:1539–1552.
- Spolar, R. S., and M. Th. Record, Jr. 1994. Coupling of local folding to site-specific binding of proteins to DNA. *Science.* 263:777–784.
- Szyperski, Th., A. Ono, C. Fernandez, H. Iwai, S. Tate, K. Wüthrich, and M. Kainosho. 1997. Measurement of the <sup>3</sup>J<sub>C2'P</sub> scalar couplings in a 17 kDa protein complex with <sup>13</sup>C, <sup>15</sup>N-labeled DNA distinguishes the B<sub>I</sub> and B<sub>II</sub> phosphate conformations of the DNA. *J. Am. Chem. Soc.* 119:9901–9902.
- Taillandier, E. 1990. Nucleic acid conformations studied by vibrational spectroscopy. In *Structure and Methods*, Vol. 3, DNA and RNA. R. H. Sarma and M. H. Sarma, editors. Adenine Press, Schenectady, NY. 73–78.
- Taillandier, E., and J. Liquier. 1992. Infrared spectroscopy of DNA. *Methods Enzymol.* 211:307–335.
- Vandeginste, B. G. M., and L. De Galan. 1975. Critical evaluation of curve fitting by infrared spectrometry. *Anal. Chem.* 47:2124–2132.
- Travers, A. 1994. DNA-Protein Interactions. Chapman and Hall, New York.
- Winger, R. H., K. R. Liedl, S. Rüdissler, A. Pichler, A. Hallbrucker, and E. Mayer. 1998. B-DNA's B<sub>I</sub> → B<sub>II</sub> conformer substate dynamics is coupled with water migration. *J. Phys. Chem. B.* 44:8934–8940.